Coupling between elasticity in a nematic phase and front dynamics for a moving nematic-isotropic boundary

Chaouqi Misbah and Alexandre Valance
Laboratoire de Spectrométrie Physique, Université Joseph Fourier, Grenoble I, Centre National de la Recherche Scientifique, Boîte Postale 87, 38402 Saint-Martin d'Heres, France
(Received 7 June 1994)

During growth or melting of the nematic phase at the expense of the isotropic one caused by pulling the sample from a hot into a cold thermal contact, or vice versa (directional ordering or melting), the two-phase front undergoes a morphological instability on the mesoscale at a critical pulling speed, known under the name of the Mullins-Sekerka instability. Their original work [J. Appl. Phys. **35**, 444 (1964)] focused on the diffusive nature of the instability: it is driven by impurity diffusion. At large speeds—where the destabilizing diffusion length is small enough—the front restabilizes into a planar one due to surface tension. The anchoring of the liquid crystal molecules on both the front and the plates within which the sample is confined causes strong distortions of the molecules, which react on front dynamics. In this paper, we present a general formulation for the coupling between elasticity in a nematic phase and front dynamics during growth or melting of the nematic phase. As an exploitation of this model, we confine ourselves to a simplistic geometry of the director configuration in the linear regime (where the front depletion is small). We find that both during growth and melting, the coupling leads to a drift of the pattern along the two-phase front. During melting, and at large enough growth velocities (which are experimentally accessible and lie in the range 100–200 μm/s), the coupling is stong and leads to a large shift of the restabilization speed. We present the results in a physically appealing picture. Speculation and outlook for new lines of physical inquiries are presented.

PACS number(s): 61.50.Cj, 81.30.Fb., 05.70.Fh

I. INTRODUCTION

When a solid or a liquid crystal is directionally grown (i.e., pulled at a constant speed V in an applied thermal gradient) or dissolved, the planar front is susceptible to a morphological instability, first analyzed by Mullins and Sekerka [1]. Since their original work, the problem of pattern formation in crystal growth has shown impressive development both theoretically and experimentally. A recent renewed interest was stimulated thanks to growth experiments on a nematic phase by Simon, Bechhoefer, and Libchaber [2], which revealed various symmetry-breaking bifurcations, such as parity breaking of the cellular structure. An important insight toward the understanding of the growth processes has been recently achieved by focusing on the large speed regime, where the front equation turns out to be more tractable. Numerical along with analytical efforts have shown that an initially cellular steady-state pattern may undergo a cascade of symmetry-breaking bifurcations, leading ultimately to transition to chaos [3–5].

Despite the considerable amount of knowledge that has been accumulated, a full understanding of the various experimentally pertinent ingredients in liquid crystal systems is far from being acquired. For example, following an experimental observation on an extended traveling mode during growth of a nematic phase by Simon and Libchaber [6], Oswald [7] devised an experiment that showed that such a mode was induced by the configuration of the director in the liquid crystal. Moreover, Simon and Libchaber [8] observed in a subsequent experiment, a new mode of growth where the cells execute a collective oscillatory tilting: The whole cellular pattern tilts to, say, the right, and then to the left, and so on. The observed propagation velocity along the front is so high that it is natural to attribute it to the sound speed in the nematic phase. These phenomena clearly point to the fact that elasticity in the nematic phase is very active in the process by which patterns are formed.

The main objective of this work is to formulate the growth problem in the presence of elasticity. In order to make contact with the theory, we shall first exploit the model by confining ourselves to a simple geometry of the director in the linear regime. Nonlinear effects, along with a more realistic director topology, will be the subject of a future work.

An important result to emerge from our analysis is that coupling between elasticity and front dynamics is strong. In the simplistic configuration we have considered, namely that the director makes a fixed angle with the front, we find that (i) during growth, the coupling leads to a drift of the pattern and that (ii) during melting, besides the drift, the coupling significantly shifts the restabilization velocity.

Here is a brief survey of the presentation. In Sec. II we present the full growth equations. We shall then specialize the model to some situations, such as a one constant approximation in the Frank-Oseen free energy. In Sec. III, we consider a simple director configuration and characterize the planar front solution. We then analyze, in Sec. IV, the linear stability analysis for growth. In Sec. V, we deal with melting. The summary together with outlooks will be presented in Sec. VI.

II. BASIC FORMULATION

We consider the standard directional setup. A sample is pulled in the z direction at a constant speed V. We shall consider an extended geometry, so that in a first level we will disregard the anchoring problem on the plates, within which the sample is confined. We shall come back to this point in Sec. VI.

In the isotropic phase, the equations of motion are the standard ones. As usual we neglect heat transport, hydrodynamics, and assume identical thermal properties of both phases. Let $z=\zeta(x,t)$ designate the instantaneous front position. The sample is pulled at a constant speed V in an external thermal gradient G. Mass conservation in the isotropic phase reads (in the laboratory frame)

$$\frac{\partial C_L}{\partial t}-V\frac{\partial C_L}{\partial z}=D_L\nabla^2 C_L \ , \tag{1}$$

where C_L is the impurity concentration and D_L the diffusion constant.

To deal with the nematic phase, let us first consider the motion of the director, which is specified by the unit vector $\mathbf{m}(\mathbf{r},t)$. Its equation can be written in the general form from conservation of the angular momentum [9–12].

$$I\frac{d\boldsymbol{\Omega}}{dt}=\boldsymbol{\Gamma}_F+\boldsymbol{\Gamma}_{\rm visc} \ . \tag{2}$$

The term on the left-hand side is the inertial one: I is the inertial momentum per unit volume and $\boldsymbol{\Omega}=\mathbf{m}\times(d\mathbf{m}/dt)$ is the angular velocity. The second term on the right-hand side of (2) represents the viscous term and is given by

$$\boldsymbol{\Gamma}_{\rm visc}=-\gamma_1\mathbf{m}\times\frac{d\mathbf{m}}{dt} \ , \tag{3}$$

where γ_1 is the shear viscous coefficient. The first term on the right-hand side of Eq. (2) represents the elastic force contribution to the torque, and is given by

$$\boldsymbol{\Gamma}_F=-\mathbf{m}\times\mathbf{h} \ , \tag{4}$$

where $\mathbf{h}$ is the so-called molecular field, and is nothing but the functional derivative of the Frank-Oseen free energy, F

$$h_i\equiv\frac{\delta F}{\delta m_i}=\frac{\partial F}{\partial m_i}-\frac{\partial}{\partial x_j}\frac{\partial f}{\partial(\partial_j m_i)} \ . \tag{5}$$

f is the free energy density given by

$$f=\tfrac{1}{2}K_1(\mathrm{div}\mathbf{m})^2+\tfrac{1}{2}K_2(\mathbf{m}\cdot\mathrm{rot}\mathbf{m})^2+\tfrac{1}{2}K_3(\mathbf{m}\times\mathrm{rot}\mathbf{m})^2 \ , \tag{6}$$

where K_1, K_2, and K_3 are the elastic constants, representing splay, bend, and twist deformations, respectively. Note that repeated indices are to be summed over.

Actually, for the practical purposes, the inertial term in (2) is negligibly small. Indeed $I=\rho a^2$, where $\rho(\sim 1$ g/cm^3) is the density and $a(\sim 20$ Å) is the length of the molecule. Therefore, the inertial term $\sim 10^{-12}$ ω^2 g/cm^3 (where ω is a typical rotation frequency of the director). This term is to be compared to $\gamma_1\omega$ (the viscous term). Typically $\gamma_1\sim 0.1-1$ g/(cm^3 s). Therefore, as long as one is interested in not too high frequencies ($\omega\ll 10^{10}$ s^{-1}, which are too high values in growth experiments) we can safely neglect the inertial term. The final form of the director equation can then be written as [by using (2)–(6)]

$$\gamma_1\frac{d\mathbf{m}}{dt}+\mathbf{h}=\beta\mathbf{m} \ , \tag{7}$$

where β is a Lagrange multiplier that enforces $\mathbf{m}^2=1$.

Here we shall restrict ourselves to a situation where the system is invariant in the direction orthogonal to the plates (i.e., the y direction). This implies that twist deformations are absent ($\mathbf{m}\times\mathrm{rot}\mathbf{m}=\mathbf{0}$). Moreover, we limit ourselves to a one constant approximation $K_1=K_2=K_3=K$. Under these assumptions, the molecular field takes the form

$$h_x=-K\left[\frac{\partial^2 m_x}{\partial x^2}+\frac{\partial^2 m_x}{\partial z^2}\right] \ , \quad h_z=-K\left[\frac{\partial^2 m_z}{\partial x^2}+\frac{\partial^2 m_z}{\partial z^2}\right] \ , \tag{8}$$

so that each component ($i=x,z$) of the director obeys the following simple equation:

$$\gamma_1\frac{\partial m_i}{\partial t}-K\left[\frac{\partial^2 m_i}{\partial x^2}+\frac{\partial^2 m_i}{\partial z^2}\right]=\beta m_i \ . \tag{9}$$

The director dynamics equations are better expressed in terms of the angle ϕ defined by $m_x=\sin(\phi)$ and $m_z=\cos(\phi)$. It is then easy to see from Eq. (9) that ϕ obeys (in the laboratory frame moving in the z direction at velocity V with respect to the sample)

$$\gamma_1\left[\frac{\partial\phi}{\partial t}-V\frac{\partial\phi}{\partial z}\right]=K\nabla^2\phi \ . \tag{10}$$

Let us now deal with the mass diffusion problem. The impurity concentration in the nematic phase obeys the following equation

$$\frac{\partial C_S}{\partial t}-V\frac{\partial C_S}{\partial z}=\mathrm{div}[D_\perp\nabla C_S+D_a(\mathbf{m}\cdot\nabla C_S)\mathbf{m}] \ , \tag{11}$$

which involves the nematic anisotropy. The quantity $D_a=D_\parallel-D_\perp$, where $D_\parallel$ and $D_\perp$ are the diffusion constants along and perpendicular to the molecules, respectively. At the interface we must require continuity of mass transport, which amount to

$$(D_\perp\nabla C_S-D_L\nabla C_L)\cdot\mathbf{n}+D_a(\mathbf{m}\cdot\nabla C_S)\mathbf{m}\cdot\mathbf{n}=-(C_S-C_L)\mathbf{v}\cdot\mathbf{n} \ , \tag{12}$$

where $\mathbf{n}$ is the normal vector pointing into the isotropic phase and $\mathbf{v}\cdot\mathbf{n}$ is the normal growth velocity. The boundary conditions must be supplemented with the chemical condition at the interface. For a molecularly rough interface, we assume local chemical equilibrium. Then, expanding the chemical potentials for the binary mixture about a reference point, we find [13]

$$C_S=kC_L \ , \tag{13}$$

$$G\zeta+T_0=\left[1-\gamma\frac{\kappa}{L}\right]T_M+m_L C_L-2\frac{T_M}{L}n_i t_{ij} n_j \ , \qquad (14)$$

where k is the segregation coefficient, T_M the melting temperature, γ the surface tension, L the latent heat per unit volume, m_L the liquidus slope, and t_{ij} the stress tensor given by

$$t_{ij}=-\frac{\partial f}{\partial(\partial_i m_k)}\partial_j m_k+\alpha_2 m_i\frac{\partial m_j}{\partial t}+\alpha_3 m_j\frac{\partial m_i}{\partial t} \ . \qquad (15)$$

α_2 and α_3 are the Leslie coefficients [14,15]. Equation (14) is the modified Gibbs-Thomson condition in the presence of elasticity. Actually, for situations where the temperature is not too high, $t_{ij}\ll L$. Indeed, $t_{ij}\sim K/d^2$, where d is a typical scale for the director deformation (say, of the order of a μm, while $K\sim 10^{-12}$ N), so that $t_{ij}\sim 10^{-4}$ J cm^{-3}. Since $L\sim 1-10$ J/cm^3, this contribution can safely be neglected.

Finally we must specify the other boundary conditions. First, the concentration far ahead of the interface is maintained at $C_L=C_\infty$. The other condition is a new one: It expresses how the director behaves at the interface. Contrary to what happens for liquids or solids, in liquid crystals we may have the situation where the surface energy fixes the large scale behavior, while the bulk elastic energy fixes that of short scales! (Think of a droplet. At short scales, the surface energy dominates. The form is spherical, while at large scales gravity makes it flatter, which may just be the opposite for liquid crystals!) To see this, it suffices to compare the surface energy to the bulk energy. Without loss of generality, consider only pure bend deformations (actually the following reasoning is rather dimensional, and the present assumption is irrelevant). Then the bulk elastic energy is simply $F_{\rm bulk}\sim\int K_2(\partial\theta/\partial y)^2 dy$ (y is the axis along which the torsion takes place). If d designates the typical length for the director deformation, then we have $F_{\rm bulk}\sim K_2/d$. The pinning of the director at the surface is characterized by a certain energy of interaction with the interface, so that $F_{\rm surf}=A=$const. (It has a dimension of an energy per unit surface.) This implies that $F_{\rm bulk}/F_{\rm surf}\sim K_2/dA$. One thus sees that at large scales $d\gg d^*=K_2/A$ surface energy prevails, while at short scales the bulk energy dominates. One expects *a priori* d^* to be of the order of molecular scales. Indeed K_2 (from a purely dimensional analysis) is a molecular interaction energy U divided by a molecular length a, U/a, whereas $A\sim U'/a^2$, where U' is the director-"wall" energy interaction (the wall is the isotropic phase). Contrary to what might happen with a chemically treated real wall, here the involved energy interaction U' is expected to fall in the same range as U, so that $d^*\sim a$, a molecular scale. As $d\gg d^*$, one may be in a situation where surface energy prevails. That is to say the director is—down to some scale (see below)—pinned at the interface, while the director in the bulk should accommodate to obey such a pinning. The condition on $\mathbf{m}$ at the front is simply given by

$$\mathbf{m}\cdot\mathbf{n}=\cos(\phi_0) \ , \qquad (16)$$

where ϕ_0 is the pinning angle, reflecting the details of the (anisotropic) interaction of the director with the interface.

A remark is necessary before proceeding further. We must mention here that the fact that we take, for the evaluation of A, a length of the order of the molecular length is only dictated by intuition. Some experiments [16,17] reported that the interface thickness is about 100 Å. Thus, if one uses this value in the evaluation of the interface energy instead, one finds that $d^*\sim 1$ μm, a scale that may become comparable to the pattern wavelength. That is to say, that below this scale we expect both energies to contribute. However, in view of experimental observations [16], we can still say that the angle, up to scales of the order of 100 Å, points in a preferred direction, as represented by Eq. (16).

The set of Eqs. (1)–(16) completely describes the general front dynamics coupled to the nematic elasticity, which we shall now treat in some specific cases. Before going further, let us mention that K/γ_1, which has the dimension of a viscosity (or a diffusion coefficient), is in the range 10^{-6}–10^{-7} cm^2/s, which is of the order of the impurity diffusion constant, $D\sim 10^{-7}$ cm^2/s for the nematic liquid crystal 8CB [which is in a homologous series of 4-cyano-4′-(n-alkyl)biphenyl liquid crystals] [18]. Therefore, we expect the coupling between elasticity and growth dynamics to be important.

We find it convenient to introduce dimensionless quantities

$$x=\frac{\tilde{x}}{l} \ , \quad z=\frac{\tilde{z}}{l} \ , \quad \zeta=\frac{\tilde{\zeta}}{l} \ , \quad t=\frac{\tilde{t}}{\tau} \ , \qquad (17)$$

$$u=\frac{C-C_\infty}{\Delta C} \ , \quad T=\frac{\tilde{T}}{\Delta T} \ , \qquad (18)$$

where $l=2D_L/V$, $\tau=l^2/D_L$, $\Delta C=[(1-k)/k]C_\infty$, and $\Delta T=|m_L|\Delta C$. The variables with tildes refer to the physical ones. The full equations of motion become then

(i) isotropic phase

$$\nabla^2 u_L+2\frac{\partial u_L}{\partial z}=\frac{\partial u_L}{\partial t} \ , \qquad (19)$$

(ii) crystalline phase

$$\nu_\perp\nabla^2 u_S+2\frac{\partial u_S}{\partial z}+\nu_a\nabla\cdot[(\mathbf{m}\cdot\nabla u_S)\mathbf{m}]=\frac{\partial u_S}{\partial t} \ , \qquad (20)$$

(iii) interface

$$(\nu_\perp\nabla u_S-\nabla u_L)\cdot\mathbf{n}+\nu_a(\mathbf{m}\cdot\nabla C_S)\mathbf{m}\cdot\mathbf{n}=-(u_S-u_L)\left[2+\frac{\partial\zeta}{\partial t}\right]n_z \ , \qquad (21)$$

where $\nu_\perp=D_\perp/D_L$ and $\nu_a=D_a/D_L$. The director Eq. (10) takes the form

$$\frac{\partial\phi}{\partial t}=\eta\nabla^2\phi+2\frac{\partial\phi}{\partial z} \ , \qquad (22)$$

where $\eta=K/D_{L\gamma 1}$. This equation is subject to the pinning condition

$$\mathbf{m}\cdot\mathbf{n}=\cos(\phi_0) \ . \qquad (23)$$

Finally, the local equilibrium equations [Eqs. (13) and (14)] read

$$u_S = k(u_L - 1) , \tag{24}$$

$$u_L = 1 - \frac{\zeta}{l_T} d_0 \kappa , \tag{25}$$

where $l_T^{-1} = lG/\Delta T$ is the thermal length and $d_0 = \gamma \tilde{T}_M / lL\Delta T$ the capillary length. Note that both lengths are reduced by the diffusion length l.

III. PLANAR FRONT SOLUTION

The set of Eqs. (20)–(25) admits a planar front solution moving at a constant speed V. The front position will be taken at $z=0$. The director Eq. (22) subject to (23) is solved by $\phi = \phi_0$, that is to say the director is uniform ($\mathbf{m} = \mathbf{m}^0$). The diffusion field is simply given by

$$u_s = 0 , \quad z < 0 , \tag{26}$$

$$u_L = e^{-2z} , \quad z > 0 . \tag{27}$$

The concentration field is exactly the same as the one without elasticity. This is a result of the fact that for growth, the diffusion field in the nematic phase is constant; there is no diffusion current. We shall see that this is not the case during melting.

IV. LINEAR STABILITY ANALYSIS

We study regression of fluctuations by looking for solutions of the form

$$\zeta(x,t) = \varepsilon e^{iqx + \omega t} , \tag{28}$$

where q is the wave number and ω the amplification (or attenuation) rate that we wish to determine. The response of the bulk fields is written as

$$\delta \mathbf{m} = \mathbf{m} - \mathbf{m}^0 = \varepsilon \mathbf{m}^1(z) e^{iqx + \omega t} , \tag{29}$$

$$\delta u_L = u_L - u_L^0 = \varepsilon u_L^1(z) e^{iqx + \omega t} , \tag{30}$$

$$\delta u_S = u_S = u_S^0 = \varepsilon u_S^1(z) e^{iqx + \omega t} . \tag{31}$$

The response of the director to the perturbation is written in terms of ϕ as

$$\delta\phi = \phi - \phi_0 = \varepsilon \phi_1(z) e^{iqx + \omega t} . \tag{32}$$

Inserting this expression into Eq. (22), we obtain

$$\phi_1(z) = A e^{\mu z} , \tag{33}$$

where

$$\mu = -[1 - (1 + \eta\omega + \eta^2 q^2)^{1/2}]/\eta . \tag{34}$$

A is an integration constant that is easily obtained from the pinning condition [Eq. (23)] to be $A = -iq$.

Inserting (30) and (31) into (19) and (20), neglecting all but linear terms in ε, we obtain two equations for u_L^1 and u_S^1, the solutions of which are

$$u_L^1(z) = A_L e^{-\mu_L z} , \tag{35}$$

$$u_S^1(z) = A_S e^{\mu_S z} , \tag{36}$$

where

$$\mu_L = 1 + (1 + \omega + q^2)^{1/2} , \tag{37}$$

$$\mu_S = \left\{ -(1 + i\nu_a q \cos\phi_0 \sin\phi_0) + [(1 + i\nu_a q \cos\phi_0 \sin\phi_0)^2 + (\nu_\perp + \nu_a \cos^2\phi_0)(\omega + (\nu_\perp + \nu_a \sin^2\phi_0) q^2)]^{1/2} \right\} (\nu_\perp + \nu_a \cos^2\phi_0)^{-1} . \tag{38}$$

A_L and A_S are integration constants. Using the boundary conditions [Eqs. (21), (24), and (25)] to order ε, we find

$$A_L = 2 - l_T^{-1} - d_0 q^2 , \tag{39}$$

$$A_S = -k(l_T^{-1} + d_0 q^2) , \tag{40}$$

$$\omega = A_S[(\nu_\perp + \nu_a \cos^2\phi_0)\mu_S + i\nu_a q \cos\phi_0 \sin\phi_0] + A_L[\mu_L + 2(k-1)] - 4k . \tag{41}$$

Combining these equations and using the definitions (37) and (38), we obtain the following dispersion relation:

$$\omega = -2 - (l_T^{-1} + d_0 q^2) \times [1 + (\nu_\perp + \nu_a \cos^2\phi_0)\omega + (\nu_\perp^2 + \nu_\perp \nu_a) q^2 + 2i\nu_a q \cos\phi_0 \sin\phi_0]^{1/2} + (2 - l_T^{-1} - d_0 q^2)(1 + \omega + q^2)^{1/2} , \tag{42}$$

where we have set $k = 1$. Note that elasticity does not play a role at this order; the parameter η [which characterizes nematic distorsions; its definition is given after (22)] is absent from the present dispersion relation. The effect of the director enters via anisotropy only. The new feature is that at the Mullins-Sekerka threshold, the spectrum contains an imaginary part, which should manifest itself by a drift of the structure transversely to the front.

In this section we shall confine ourselves to the low-velocity regime, where $q \gg 1$ (recall that q is reduced by the inverse of the diffusion length). In this limit, an expansion to leading order in q of (42) yields

$$\omega_R \approx -2 + [2 - (1 + \sqrt{\nu_\perp \nu_\parallel}\, l_T^{-1})] q + (1 + \sqrt{\nu_\perp \nu_\parallel}) d_0 q^3 , \tag{43}$$

$$\omega_I \approx -\frac{\nu_a \cos\phi_0 \sin\phi_0}{\sqrt{\nu_\perp \nu_\parallel}} (l_T^{-1} + d_0 q^2) , \tag{44}$$

where we have introduced the real and imaginary parts of ω, ω_R, and ω_I. At the bifurcation point (defined by $\omega_R=0$ and $\partial\omega_R/\partial q=0$). The critical condition for the onset of the instability, and the critical wave number are given from (43) by

$$(l_T^{-1})_c=\frac{2}{(1+\sqrt{\nu_\perp\nu_\parallel})}\ , \tag{45}$$

$$q_c^2=\left[\frac{1}{(1+\sqrt{\nu_\perp\nu_\parallel})d_0}\right]^{2/3}\ . \tag{46}$$

At the bifurcation point ω_I is easily obtained from (44), and thus the drift velocity ($V_d=\omega_I/q_c$) reads

$$V_d=\frac{\omega_I}{q}=-\frac{2\nu_a\cos\phi_0\sin\phi_0}{\sqrt{\nu_\perp\nu_\parallel}(1+\sqrt{\nu_\perp\nu_\parallel})}\ . \tag{47}$$

Recall that this velocity is reduced by the pulling speed. Its magnitude is fixed by that of the pinning angle. Since, generically, ϕ_0 is finite, the physical drift velocity is a noticeable fraction of the pulling speed. Note also that V_d vanishes for two special situations: (i) If $\nu_a=0$ (recall that $\nu_a\sim D_\parallel-D_\perp$). This is what we could expect, since during growth the presence of a nematic phase manifests itself via anisotropy. In the purely isotropic case, there should be thus no effect of the nematic phase. (ii) If $\phi_0=0$ or $\phi_0=\pi/2$ (modulo π). This is also what we could have *a priori* expected. In the first case, this means that the molecules are perpendicular to the front, while in the second case, they are parallel to it. Since the present drift is induced by the loss of right-left symmetry (due to the pinning in a preferred direction), it is clear that for $\phi_0=0,\pi/2$ the reflexion symmetry about the growth axis is restored and the drift disappears. Of course, we could not exclude the fact that the coupling between elasticity and the front dynamics leads to a Hopf bifurcation. However, since there is no zeroth-order diffusion current, one expects the coupling to be directly related to anisotropy; that is to say that in the situation where $\phi_0=0,\pi/2$, the bifurcation is expected to be stationary. This expectation is not obvious, however, in the case of melting (see next section).

V. MELTING

The front dynamics equations in this situation are of course those presented in the preceding section, after substituting the drift velocity V by $-V$. We must keep in mind, however, that this is true only in the context we are considering: The contact with the glass plates is disregarded (see Sec. VI). As shown experimentally by Bechhoefer [18], the contact with the plates may significantly affect an asymmetry between growth and melting. This remark may lead to further future investigations with the aim of clarifying the dynamics of wetting in such systems.

In order to keep the reference front position at $z=0$, we must choose the temperature origin not at $T=T_M+m_LC_\infty/k$ (as we did in the case of growth) but at $T=T_M+m_LC_\infty$. We do not find it worthwhile to rewrite the equations, but directly write the main lines of the solutions. In the planar front configuration, we find (by keeping the same notations as for growth)

$$u_L=0\ ,\quad z>0\ , \tag{48}$$

$$u_S=-ke^{2z/(\nu_\perp+\nu_a\cos^2\phi_0)}\ ,\quad z<0\ . \tag{49}$$

In the linear regime, the angle deviation ϕ_1 reads

$$\phi_1(z)=-iqe^{\mu z}\ , \tag{50}$$

where

$$\mu=[1+(1+\eta\omega+\eta^2q^2)^{1/2}]/\eta\ . \tag{51}$$

The diffusion fields in both phases are given by

$$u_L^1(z)=A_Le^{-\mu_Lz}\ , \tag{52}$$

$$u_S^1(z)=A_Se^{\mu_Sz}+Be^{Mz}\ , \tag{53}$$

where

$$\mu_L=-1+(1+\omega+q^2)^{1/2}\ , \tag{54}$$

$$\mu_S=\{(1-i\nu_aq\cos\phi_0\sin\phi_0)[(1-i\nu_aq\cos\phi_0\sin\phi_0)^2+(\omega+(\nu_\perp+\nu_a\sin^2\phi_0)q^2)(\nu_\perp+\nu_a\cos^2\phi_0)]^{1/2}\}(\nu_\perp+\nu_a\cos^2\phi_0)^{-1}\ , \tag{55}$$

$$M=\mu+\frac{2}{\nu_\perp+\nu_a\cos^2\phi_0}\ , \tag{56}$$

and B, which raises from the inhomogeneous solution of the diffusion field in the nematic phase due to the presence of a zeroth-order current, is given by

$$B=\frac{2ik\nu_aq}{(\nu_\perp+\nu_a\cos^2\phi_0)^2}\{2\cos\phi_0\sin\phi_0[2+(\nu_\perp+\nu_a\cos^2\phi_0)\mu]+iq\cos(2\phi_0)(\nu_\perp+\nu_a\cos^2\phi_0)\}$$

$$\times[(\nu_\perp+\nu_a\cos^2\phi_0)M^2-2(1-i\nu_aq\cos\phi_0\sin\phi_0)M-(\omega+(\nu_\perp+\nu_a\sin^2\phi_0)q^2)]^{-1}\ . \tag{57}$$

The general dispersion relation is given in the Appendix. Here we shall write its expression in the simple case where $\phi_0=0$. We have already seen that $\phi_0\neq 0$ induces a drift of the pattern. Since in the present case the coupling between elasticity and the front is not trivial—due to the presence of a zeroth-order diffusion field in the nematic phase—we find it useful not to analyze simultaneously all the effects. We shall, therefore, for sake of clarity, focus on the situation where $\phi_0=0$. In this limit, the dispersion relation reads

$$\omega=-\frac{2}{\nu_\parallel}+\left[\frac{2}{\nu_\parallel}-l_T^{-1}-d_0q^2\right](1+\nu_\perp\nu_\parallel q^2+\nu_\parallel\omega)^{1/2}-(l_T^{-1}+d_0q^2)(1+q^2+\omega)^{1/2}+\frac{+2\nu_a q^2[\nu_\parallel\mu+1-(1+\nu_\perp\nu_\parallel q^2+\nu_\parallel\omega)^{1/2}]}{\nu_\parallel^2\mu^2+2\nu_\parallel\mu-(\nu_\parallel\omega+\nu_\parallel\nu_\perp q^2)} . \quad (58)$$

Note that ω is *a priori* complex. In the pure Mullins-Sekerka limit, the *principle of exchange of stability* holds [19] (that is, $\omega_R=0$ implies automatically that $\omega_I=0$). Here, due to the complexity of the dispersion relation, it has not been possible to establish whether the bifurcation is of Hopf type or not in the general case. However, both in the small- and large-velocity regimes, we can easily show that the bifurcation is steady (recall that if ϕ_0 is arbitrary we must always have an imaginary part representing the drift). At intermediate velocities, a numerical analysis of the dispersion relation shows—for the set of typical parameters used so far—that the same conclusion holds.

Let us now admit the stability exchange principle, and analyze the dispersion relation in the two extreme regimes. In the low-velocity regime (where $q\gg 1$), Eq. (58) yields

$$\omega=[2-(1+\sqrt{\nu_\parallel\nu_\perp})l_T^{-1}]q-(1+\sqrt{\nu_\parallel\nu_\perp})d_0q^3+\mathcal{H} , \quad (59)$$

where $\mathcal{H}$ represents higher-order terms. The effect of the coupling is clear. On the other hand, the penetration length of the direction distorsion in the nematic phase is of the order of q^{-1}. This means in physical variables that the penetration length is much smaller than the diffusion length. That is to say that there is a scale separation between the governing growth length (diffusion length) and the one associated with nematic distorsions, so that to leading order the nematic elasticity does not affect front dynamics. This explains why there is no trace of elasticity in Eq. (59). At this scale, the nematic effect shows up in the diffusion anisotropy only. In the isotropic case $\nu_\parallel=\nu_\perp=1$. We thus see from Eq. (59) that anisotropy stabilizes (destabilizes) if $\nu_\parallel\nu_\perp>1$ ($\nu_\parallel\nu_\perp<1$). A diffusing atom explores, within a typical collision time τ, a surface $S\sim D\tau$. In the anisotropic case, this surface (which is an ellipse on the average) is $S\sim\sqrt{D_\parallel D_\perp}\tau$. Thus, the condition $\nu_\parallel\nu_\perp>1$ ($\nu_\parallel\nu_\perp<1$) simply means that the surface excursion is larger (smaller) than in the isotropic case. In the first (second) case, an impurity makes longer (shorter) excursions before it responds to interface fluctuations, so that the front is more stable (unstable).

In the other extreme limit of large speeds (where $q\ll 1$), expansion of (59) to leading order in q provides us with

$$\omega=[-(1+\nu_\parallel\nu_\perp)l_T^{-1}-2d_0+\nu_\parallel\frac{1+\nu_\perp/\eta}{(1+\nu_\parallel/\eta)}]q^2 . \quad (60)$$

Elasticity is represented here by η ($\sim K$) in the last term of the dispersion relation. The presence of the nematic phase results in a renormalization of the capillary forces. In the purely isotropic case, we have $\nu_\parallel(1+\nu_\perp/\eta)/(1+\nu_\parallel/\eta)=1$, and the limit of absolute stability (attained when $l_T^{-1}\to 0$) is given by $2d_0=1$. In the presence of anisotropy, the new absolute stability limit is given by $2d_0=\nu_\parallel(1+\nu_\perp/\eta)/(1+\nu_\parallel/\eta)$. Thus, the coupling to the nematic phase may stabilize or destabilize the front depending on whether $\nu_\parallel(1+\nu_\perp/\eta)/(1+\nu_\parallel/\eta)>1$ or <1.

Figure 1 summarizes the results of the linear stability analysis where typical values of the physical parameters are used (see caption). These parameter values correspond to those given for 8CB by Bechhoefer *et al.* [20]. The full line is the usual neutral curve, the dashed and dotted ones correspond to the case where elasticity is present with two different set of parameters. Few remarks are in order. At low velocity, the effect of elasticity is weak. This is traced back—as discussed above—to the scale separation of diffusion and nematic distorsions. In the large velocity regime, distorsions penetrate far in the bulk. [The penetration length is of the order of $l/\eta\sim 10\times l$, see expressions (50) and (51), and their effect is, therefore, detected by the diffusion field.] The shift of the restabilization velocity (the upper maximum in Fig. 1) is dramatic. It can easily attain variations of a factor of 2. Thus, the coupling is far from being perturbative.

Note that the shift of the restabilization threshold is a feature that appears in the melting regime only. Thus, the experimental study of melting with the aim to analyze

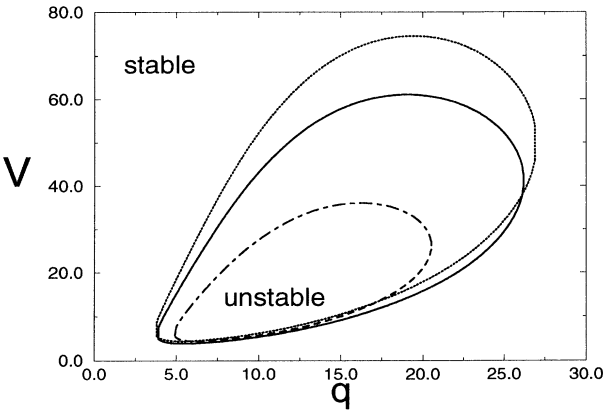

FIG. 1. The neutral curve in the plane (wave number, velocity). Full line, no anisotropy (and thus no effective coupling to elasticity). Dashed-dotted line, $\eta_\parallel=0.8$, $\eta_\perp=0.7$. Dotted line, $\eta_\parallel=1.3$, $\eta_\perp=1.2$. In all cases units are such that $l_T=1$ and $D_L=1$. In these units $d_0=0.01$ (i.e., the capillary length is 100 times smaller than the thermal length).

the restabilization regime and compare it to that of growth is crucial to guide further analysis.

VI. SUMMARY AND OUTLOOK

We have presented a general formulation of the coupling between front dynamics and elasticity in a nematic phase. This work, which is at its first stage, was motivated by various experimental phenomena, which pointed to the active role of the nematic phase in pattern selection.

In order to make contact with the formalism, we have restricted ourselves to some specific situations. We have shown that generically the coupling results in a drift of the pattern both during growth and melting. The drift velocity is a nonnegligible fraction of the pulling speed, and is thus measurable. During melting, the existence of a zeroth-order field in the nematic phase induces a nontrivial coupling. This coupling is relatively weak in the low-velocity regime. This is attributed to the weak penetration of the nematic distorsion in the bulk. In the large-velocity regime—which are by now quite accessible, and are only in the range 100–200 μm/s—the coupling is strong. It results in an important renormalization of the capillary length, which shifts the planar front restabilization threshold by an amount that may reach a factor of about 2.

Note that in all our study, we did not make use of values of real physical parameters. We have simply compared the situation where elasticity is present with the purely diffusive Mullins-Sekerka theory. In order to make quantitative comparison with real situations, it is clear that one has, in the future, to focus on this question. This will be crucial for guiding further theoretical analyses.

Our calculation is linear. It is imperative to deal with a nonlinear analysis. The first step would be to perform a weakly nonlinear analysis with the aim to study the nature of the bifurcation. Next, we must focus on the large speed regime where dynamics are quasilocal [21,22]. This is an important step that has led recently to the discovery of a myriad of patterns going from order to chaos [3–5]. Whether or not elasticity significantly affects, suppresses, or leads to new secondary instabilities within the generically ten classified instabilities [23], is a question of paramount importance that should allow us to recognize which of the instabilities—though all are potentially present from symmetry arguments—are intimately related to the underlying physics.

Our calculation was made under the assumption that the anchoring is strong at the front. This is dictated by the fact that in most cases the director has a preferred direction in the interface region—which is estimated to be of the order of 100 Å—regardless of the front depletion. This assumption seems reasonable at first sight, albeit we recognize that it is an important task for future investigations to direct research along this line in order to be more precise about this point.

The most important simplification was to disregard the presence of the plates within which the sample is confined in real situations. As already discussed, the molecules have a preferred direction at the interface. For example, for the nematic liquid crystal 8CB , the molecules lie in a cone about the interface normal, having an opening angle of about 48.5° [16]. On the other hand, the plates are usually treated in such a way that the molecules are perpendicular to them (Fig. 2). Thus, in order to simultaneously fulfill both matching conditions (at the front and the plates), a topological defect raises in the form of a disclination line (represented by the cross in Fig. 2) having a topological charge $S=-\frac{1}{2}$ [18]. Experimental observations [18] on nematic phases have revealed that such a defect may remain bound to the front as this one moves, or rather detaches from it, depending on the growth velocity. For a nonmoving front, a disclination line is subject to both repulsive and attractive forces. Indeed, the interaction of the line with its image may be repulsive or attractive depending on whether the director is strongly anchored or free to respond to the elastic force [24]. More precisely, at large enough scales (far from the front) the line is repelled by its (positive) image. Close to the surface (at short scales), however, the line is pushed towards the front. There is, thus, an interplay between these forces in the mechanism by which the defect moves. What causes the line to detach from the moving front? At present, a precise analysis is lacking. We can, nevertheless, provide an estimate about an intrinsic velocity scale—which should constitute presumably the critical velocity for the disclination—front unbinding transition. From a purely dimensional analysis, a typical velocity scale in the nematic phase—where energy dissipates due to a disclination fluctuation—is given by the combination $K/\gamma_1 d$, where K is the elastic constant, γ_1 is the shear viscosity (the Leslie) coefficient, and d is a typical length scale over which energy dissipates. Since the disclination is in part induced by the plates, it is natural to expect this scale to represent the plates spacing. Taking typical values for the nematic liquid crystal 8CB and

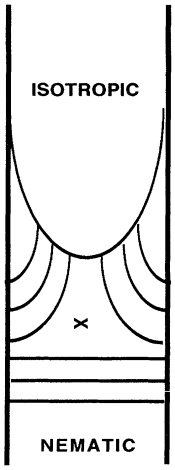

FIG. 2. A typical director configuration induced by the contact to the plates (here the molecules are perpendicular to the plates) and the pinning at the nematic-isotropic interface. These two constraints lead to a disclination line (represented by the cross).

$d \sim 50$ μm, we find this velocity to fall in the range of 10 μm/s. Although the order of magnitude is correct, the exact observed value for the line detachment is a few times bigger. Such argument, does not, on the other hand, explain the mechanism by which a disclination line detaches. It is imperative, in order to have conclusive answers, to develop a full analysis including a realistic topology of the director.

We would like to mention that the nematic-isotropic interface makes, as stated above, a well-defined polar angle with the vertical axis, whereas all the values of the azimuthal angle are equally probable. Thus, along the x coordinate we may have domains with negative and positive angles. This means, that the director topology at the front may be more complex than what we expect. We suggest that an application of a magnetic field along the x axis, which should remove the azimuthal degeneracy, constitutes an interesting test of the effect of this degeneracy. In particular, if the tilting oscillation observed by Simon and Libchaber [8] is associated with a flip-flop movement of the director at the front, the application of a magnetic field may suppress the instability, thereby providing crucial information on director dynamics.

Finally, in an interesting experiment, Oswald [7] brought out clearly the effect of elasticity on front dynamics. He concluded that both the topology of the disclination line and the elastic anisotropy strongly affect certain secondary instabilities. Moreover, Simon and Libchaber [8] discovered an interesting feature of front dynamics: At large enough velocities, and for thin enough samples, the cells collectively tilt from right to left in a permanent way. The propagation velocity seems to be much bigger than the growth velocity. It is tempting to connect this propagation with elastic properties of the nematic phase.

In conclusion, we believe that given the wide variety of fascinating physical phenomena that remain unexplained to date, the branch of research that involves elastic effects in a realistic manner, is not only a necessary step in an attempt to account for various observations, but is also an attractive line of inquiry to bring together features from the rich soft matter physics and those which pertain to nonlinear phenomena in dissipative systems.

ACKNOWLEDGMENTS

We benefited from various pertinent discussions with John Bechhoefer and Patrick Oswald.

APPENDIX

Here we list the full dispersion relation in the melting case. It can be written as

$$\begin{aligned} k\omega = {} & A_S[(\nu_\perp+\nu_a\cos^2\phi_0)\mu_S + i\nu_a q\cos\phi_0\sin\phi_0 - 2] \\ & + A_L[\mu_L + 2] \\ & + B[(\nu_\perp+\nu_a\cos^2\phi_0)M + i\nu_a q\cos\phi_0\sin\phi_0 - 2] \\ & - 2k\frac{i\nu_a q\cos\phi_0\sin\phi_0}{\nu_\perp+\nu_a\cos^2\phi_0} , \end{aligned} \tag{A1}$$

where

$$A_L = -(l_T^{-1} + d_0 q^2) , \tag{A2}$$

$$A_s = -k(l_T^{-1} + d_0 q^2 - \frac{2}{\nu_\perp+\nu_a\cos^2\phi_0}) - B , \tag{A3}$$

and

$$\begin{aligned} B = {} & \frac{2ik\nu_a q}{[\nu_\perp+\nu_a\cos^2\phi_0]^2}\{2\cos\phi_0\sin\phi_0[2+(\nu_\perp+\nu_a\cos^2\phi_0)\nu] + iq\cos(2\phi_0)[\nu_\perp+\nu_a\cos^2\phi_0]\} \\ & \times\{[\nu_\perp+\nu_a\cos^2\phi_0]M^2 - 2[1 - i\nu_a q\cos\phi_0\sin\phi_0]M - [\omega+(\nu_\perp+\nu_a\sin^2\phi_0)q^2]\}^{-1} . \end{aligned} \tag{A4}$$

In the case where $\phi_0 = 0, \pi/2$, Eq. (1) reduces to (58).

[1] W. W. Mullins and R. F. Sekerka, J. Appl. Phys. **35**, 444 (1964).
[2] A. J. Simon, J. Bechhoefer, and A. Libchaber, Phys. Rev. Lett. **63**, 2574 (1988).
[3] K. Kassner, C. Misbah, and H. Müller-Krumbhaar, Phys. Rev. Lett. **67**, 1551 (1991).
[4] K. Kassner, C. Misbah, H. Müller-Krumbhaar, and A. Valance, Phys. Rev. E **49**, 5477 (1994).
[5] K. Kassner, C. Misbah, H. Müller-Krumbhaar, and A. Valance, Phys. Rev. E **49**, 5495 (1994).
[6] A. Simon and A. Libchaber, Phys. Rev. A **41**, 7090 (1990).
[7] P. Oswald, J. Phys. (France) II **1**, 571 (1991).
[8] A. Simon and A. Libchaber (private communication).
[9] P. D. de Gennes, *The Physics of Liquid Crystals* (Oxford University Press, London, 1974).
[10] W. Helfrisch, J. Chem. Phys. **51**, 4092 (1969).
[11] Group des Cristaux Liquides d'Orsay, J. Chem. Phys. **51**, 816 (1969).
[12] W. J. A. Goossens, in *Advances in Liquid Crystal,* edited by Glenn H. Brown (Academic, New York, 1978).
[13] For an application to a similar problem (coupling between hydrodynamics and growth) see C. Misbah, thesis, Université Paris 7, 1985; see, also, B. Caroli, C. Caroli, and B. Roulet, J. Cryst. Growth **66**, 575 (1984); *ibid.* **71**, 235

(1985).
[14] F. M. Leslie, Q. J. Arch. Mech. Appl. Math. **19**, 357 (1966).
[15] F. M. Leslie, Arch. Ration. Mech. Anal. **28**, 265 (1968).
[16] S. Faetti and V. Palleschi, Phys. Rev. A **30**, 3214 (1984).
[17] J. Bechhoefer drew our attention on this question.
[18] J. Bechhoefer, Ph.D. thesis, University of Chicago, 1988.
[19] D. J. Wollkind and L. A. Segel, Philos. Trans. R. Soc. London **268**, 351 (1970).
[20] J. Bechhoefer, A. Simon, A. Libchaber, and P. Oswald, Phys. Rev. A **40**, 2024 (1989).
[21] K. Brattkus and S. H. Davis, Phys. Rev. B **38**, 11 452 (1988).
[22] A. Ghazali and C. Misbah, Phys. Rev. A **46**, 5026 (1992).
[23] P. Coullet and G. Iooss, Phys. Rev. Lett. **64**, 866 (1990).
[24] R. B. Meyer, Solid State Commun. **12**, 585 (1973).